The Procedure for Establishing the Permissible Speeds of Semi-Wagons

Seidulla Abdullayev [1], Natalya Tokmurzina-Kobernyak [1], Azamat Alpeisov [1], Arailym Tursynbayeva [1,*], Assel Kurbenova [1], Aldabergen Bektilevov [1], and Daniyar Kerimkulov [2]

[1] School of Transport Engineering and Logistics, Satbayev University, Almaty, Kazakhstan
[2] Laboratory of Intelligent Robotic Systems, Institute of Mechanics and Engineering named after Academician U.A. Dzholdasbekov, Almaty, Kazakhstan
Email: seidulla@mail.ru (S.A.); natalyatokmur@mail.ru (NT-K); alpeisov73@mail.ru (AA); nurtassovna.iqo@mail.ru (AT); a.kurbenova@satbayev.university (AK); a.bektilevov@satbayev.university (AB); Rain_forest@inbox.ru (DK)
*Corresponding author

***Abstract*—This article presents a comprehensive analysis of the permissible speeds of railway rolling stock during straight-line motion and when navigating curves with various radii. The study addresses the growing demand for higher operational speeds while maintaining safety standards and infrastructure integrity. The objective is to determine the dynamic and structural constraints that limit permissible speeds under different track conditions. The research methodology is based on analytical calculations and numerical modeling of the interaction between the rolling stock and the track infrastructure. Key factors considered include the dynamics of vehicle movement, structural strength of the metal constructions, the impact on the track, unbalanced acceleration in curves, and stability against wheel derailment. Special attention is given to the assessment of lateral forces and their influence on both vehicle and track components. The results demonstrate how permissible speeds vary with track curvature and construction characteristics. The study identifies threshold values for unbalanced acceleration and lateral forces, which serve as critical criteria for speed limitations. The findings can be applied in the design and modernization of railway vehicles, the development of infrastructure guidelines, and the formulation of regulatory standards aimed at improving operational safety and performance in railway systems.**

***Keywords*—railway track, curved section, rolling stock, locomotive wheelset, vertical dynamics, axial stresses in rails**

I. Introduction

One of the key directions for improving the efficiency of the transportation process is the development of innovative wagon designs capable of withstanding increased wheel load on the rails [1, 2]. The introduction of freight wagons with higher axle loads will allow for the solution of the problem of increasing the weight limits of freight trains without additional investments in the development of track infrastructure. To effectively develop heavy-haul transportation, it is necessary to use wagons with improved load capacity. Based on international experience, the greatest economic benefit has been achieved through the application of enhanced three-component bogies for freight wagons [3–5]. Different countries are considering increasing axle load within various limits. For example, Australia has recommended increasing the axle load to 37 tons; Canada, South Africa, and Brazil to 30 tons; the USA to 25–32.4 tons; and India, China, Russia, and Kazakhstan to 25 tons [6]. A significant increase in axle load requires work on strengthening the railway track, leading to high costs. However, an axle load up to 30 tons typically does not require substantial investments in track infrastructure. In this case, comprehensive research is necessary to assess the impact of rolling stock on railway infrastructure, as well as the development of innovative wagon designs that can minimize dynamic impact on the track.

Currently, several models of freight wagons with an axle load of 25 tons have been developed and tested, including models 18-194-1, 18-9855, 18-9810, and 18-9996 (ZK1). The bogies of model 18-9855 have significant differences from the most common bogie model 18-100 with an axle load of 23.5 tons. These bogies use side elastic sliding bearings with constant contact, the wheelsets are made of high-hardness steel, and cassette tapered bearings are used in the axlebox with support on the side frame via an adapter. Wear-resistant polymer gaskets are used in the bearing unit. These technical solutions help reduce the dynamic forces transmitted to the track. Articles [7, 8] present the results of dynamic testing of freight wagons with an axle load of 25 tons. The authors established that the dynamic impact of wagons 18-194-1, 18-9810, and 18-9996 (ZK1) lies within the established standards, with the greatest negative impact on the railway track coming from the bogies of model 18-9996 (ZK1).

Manuscript received February 7, 2025; revised April 1, 2025; accepted May 8, 2025; published September 8 , 2025.

(a) (b) (c)

Fig. 1. Types of bogies (axle load; design speed). (a) basic (25 t; 120 km/h); (b) for increased speeds (20 t; 140 km/h); (c) with a carrying capacity of (30 t; 100 km/h) [1, 2].

This article examines the impact of the 12-9920 model hopper wagons on the railway track. The design of this hopper wagon incorporates the 18-9996 (ZK1) bogie. Compared to traditional three-component freight bogies, this bogie has several structural features. It is designed for an axle load of 25 tons and a maximum speed of 120 km/h in both loaded and empty conditions see Fig. 1. The lateral spread of the wheelset relative to the side frame has been increased, which ensures better fitting in curves at higher speeds. A rubber adapter is positioned between the axle box and the side frame, which facilitates the radial installation of the wheelset in curves. Additionally, the ZK1 bogie uses diagonal connections, which eliminate instability when navigating curved track sections. A detailed description of this bogie design is provided in [9].

The novelty of this study lies in conducting and analyzing the test results of 12-9920 model hopper wagons on the railways of Kazakhstan and establishing, based on the conducted research, the safe operational conditions for these wagons and the permissible speed limits, which are reflected in the regulatory and technical documentation of the Ministry of Transport of the Republic of Kazakhstan. The current trend of increasing speeds on railways has further intensified research aimed at accurately predicting the stress-strain state of railway track elements. In these studies, the Fuchs-Winkler elastic foundation model [10–13] is primarily used. The methodology for calculating the stress-strain state of railway track under the influence of rolling stock is also based on the Fuchs-Winkler model [14, 15]. In this model, the railway track foundation is represented as a collection of independent elastic elements (springs), each responding to a load only at its point of application. The ground's reaction is proportional to the settlement. This model allows for the consideration of local soil deformations under load but does not account for the interaction between adjacent sections of the soil. This limitation does not introduce significant inaccuracies in determining the calculated load impact values on the track. According to [16–18], the main calculation algorithm for track strength (Eisenmann method) is based on the following key assumptions and premises:

- The rail is considered an uninterrupted beam of infinite length with an unchanging cross-section, resting on a continuous, equally elastic foundation;
- Vertical forces are assumed to be applied in the plane of symmetry of the rails. The rails of both tracks are assumed to be equally loaded;
- It is assumed that the wheels, during movement, do not detach from the rails and do not create impact forces;
- The calculation is based on the assumption of a linear relationship between the pressure on the unit area of the foundation and the elastic settlement it causes;
- All track characteristics used in the calculation, including permissible stresses, are considered non-random values;
- When calculating the rail's bending, the minimum possible value of the conditional yield strength of rail steel is taken as the physical allowable stress;
- Longitudinal thermal forces and cantilever forces are not directly accounted for in the calculation but are considered by a slight reduction in the physical allowable stress;
- Horizontal transverse forces and eccentric application of vertical loads are accounted for by a special factor *f*, which converts axial stresses at the rail base to stresses at its outer edge;
- The static load transmitted through the wheel to the rail is considered a non-random value; the effects of variable forces are treated as static;
- The impact of all types of vibrations from the suspension structure is considered empirically through the additional compression of the spring set and the dynamic stiffness of the suspension;
- The effects of isolated track irregularities and isolated or continuous wheel irregularities are taken into account;
- The resultant of all vertical forces, as calculated, transmitted by the wheel to the rail, is taken at its maximum value with a probability of $\Phi = 0.994$ that this value will not be exceeded;
- The internal stresses in the upper structure elements are not considered;
- The calculation is performed for a given track section when rolling stock of the same type and configuration moves along it. The calculated section is chosen where the spring compression is greatest.

Before conducting the track strength calculations, tests are carried out to determine the impact of the rolling stock on the track and switches. During these tests, the following parameters of the rolling stock are determined: vertical dynamic coefficient related to the wheel weight of the unsprung parts; the coefficient of transition from axial stresses at the rail base to edge stresses *f*, which accounts for the impact of horizontal forces on the rail and the eccentricity of vertical load application; the dynamic axle load; the stability coefficient against wheel derailment. The methodology for determining the transition coefficient from axial stresses at the rail base to edge stresses *f* is detailed in [19]. This document defines the permissible levels of impact indicators of railway rolling stock on the track and switches, as well as experimental and calculation methods for determining the impact indicators of railway rolling stock on the railway track when the rolling stock

moves at speeds of up to 250 km/h on 1520 mm gauge railway tracks (see Fig. 1) [20].

II. Materials and Methods

Comprehensive Dynamic and Track Impact Testing of Rolling Stock involves tests during which dynamic processes are simultaneously recorded both on the rolling stock and in the elements of the track superstructure, as well as in the elements of switch points [21]. Before being put into operation, rolling stock undergoes various types of testing to ensure it meets the required safety and performance criteria, after which it is permitted to operate on mainline tracks of general use. These tests define permissible levels of impact that rolling stock can exert on the track and switch points, as well as the methods for accurately determining these impact indicators [22].

Tests are conducted to determine the actual values of impact indicators during various types of testing of new, upgraded, or in-service rolling stock. During comprehensive dynamic tests and tests on the wagon's impact on the track, fixed straight and curved sections of track of limited length are generally selected, which are equipped with appropriate measuring instruments to determine rail stresses, rail bending under the influence of transverse horizontal forces from the wagon, stress on the main earthwork platform, and forces from the rails on the ties and ballast. During dynamic tests of wagons, the following values and processes are measured and recorded using special instruments:

Vertical and transverse (sometimes longitudinal) horizontal accelerations of the wagon body in the body bolster area (for passenger cars, also in the middle part of the body) and on the bogie frame; Transverse horizontal (frame) forces acting from the wheelsets on the bogie frame. Tests of the 12-9920 model hopper wagons were conducted in the Republic of Kazakhstan on various sections of railway track: Straight track section (Berlik–Zhidele, km 1489-1502, even track); Curve with a radius of 400 m (Chokpar–Alaygyr, km 3817-3818, odd track). The tests were conducted in accordance with the testing program PN-0118-2016 [23, 24].

Before the operational tests, the hopper wagons were equipped with strain gauges assembled into special measurement circuits to measure the dynamic vertical coefficients of the first and second stages of the suspension system, as well as frame forces. The strain gauges were attached to the side walls and suspension beams of the hopper wagons. To determine the accelerations of the bogie and body, as well as ride smoothness indicators, accelerometers were installed Fig. 5.

Signals from all used sensors were transmitted via cables to the input of the measurement system and recorded on the hard drive of a portable computer. For the subsequent ability to measure the dynamic vertical coefficients of the first and second stages of the suspension system, after equipping the hopper wagons with strain circuits, static tests were carried out during which the static load from the wagon body to the bogie was determined at the locations of the strain circuits. Additionally, a special loading device was used to calibrate the frame force measurement circuits.

The sensor placement diagram is shown in Fig. 2 [25].

Ram: Frame Force Measurement Circuit;

KD I l, KD I p: Measurement Circuits for the Vertical Dynamic Coefficients of the First Stage;

KD II: Measurement Circuits for the Vertical Dynamic Coefficient of the Second Stage;

Yt, Zt, Yk, Zk: Accelerations of the Bogie Frame and Wagon Body in the Transverse and Vertical Directions (see Fig. 2).

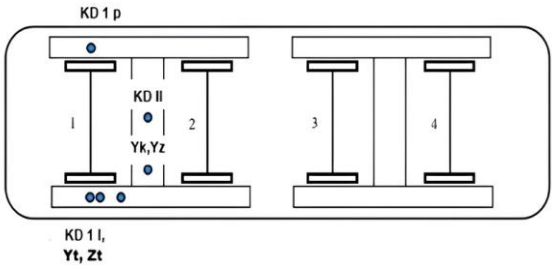

Fig. 2. Sensor placement for registering processes to determine dynamic indicators of the 12-9920 hopper wagon.

Fig. 3 shows the oscillogram of the primary measurements of dynamic processes recorded during movement along the straight track section.

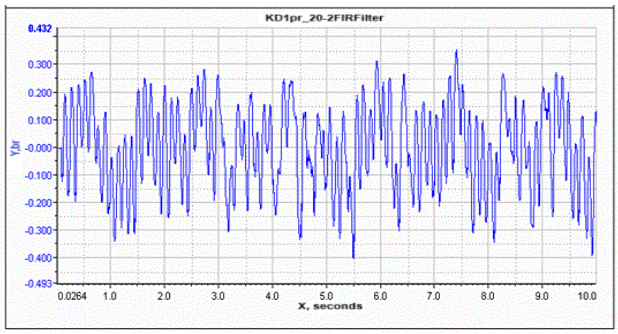

Fig. 3. Vertical dynamic coefficient of the first stage of the suspension system of the 12-9920 Hopper wagon during movement along the straight track section [26].

For measuring stresses at the rail edge of rail elements, strain gauges are used that meet established technical requirements and specifications for such devices [27]. Stress measurements are performed using strain gauge circuits with temperature compensation, formed on the outer and inner edges of the rail base in one transverse section of the rail. Active strain gauges are oriented parallel to the longitudinal axis of the rail, while the compensation gauges are oriented perpendicular to the longitudinal axis of the rail.

Active strain gauges are attached at a distance of 2 to 5 mm from the outer and inner edges of the rail base. The number of measurement sections on one rail of a 25-meter rail joint is at least 12. The method (Fig. 4) is based on the use of a direct proportional relationship between lateral forces and the difference in bending moments acting on symmetrically located points A and C of the rail cross-section relative to the neutral axis. A

complete Wheatstone bridge with temperature self-compensation is used as the measuring device.

The diagram directly determines the lateral forces in the local coordinate system of the rail and theoretically cannot introduce a significant error due to the presence of eccentricity *e*. The locations of the sensors on the track sections are shown in Fig. 5. The measurement data obtained during the movement of hopper wagons in different directions were processed separately. The records were grouped by speed and by different processes. For each process, data arrays were obtained that characterize the impact on the track of each wheelset of the hopper wagon separately, depending on the speed. The resulting data arrays were subjected to statistical processing.

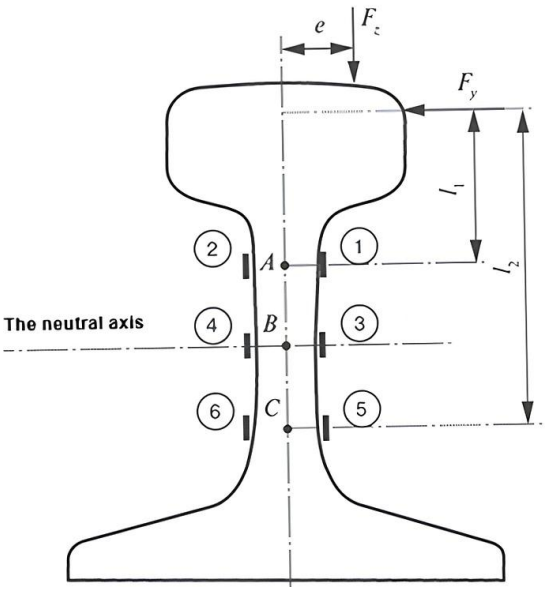

Fig. 4. Diagram of locations of strain gauges on the rail web: 1–6: strain gauge numbers; Fy: lateral force; Fz: vertical force; e: eccentricity; l1, l2: distances from the plane of application of the lateral force Fy to points A and C of the rail cross-section [25].

Numerous experimental studies show that the variation series of the stress distribution in the lower edges of the rail base, caused by the passage of the hopper wagon over the rail, follows a normal or generalized normal distribution. For the obtained set of values, the maximum probable values of the quantity are determined with a probability of 0.994. The distinctive feature of stress processing in the edges of the rail base on the straight track section is that data for both rail tracks are combined into one series. Meanwhile, the stresses in the outer and inner edges of the rail base are processed separately. Fig. 6 shows the oscillograms of the primary measurements of the impact on the track, recorded during movement along the straight track section.

The establishment of permissible speeds for the movement of semi-wagons model 12-9920 based on track strength. The determination of the permissible speed of rolling stock movement based on track strength conditions is carried out in accordance with the Methodology for Assessing the Impact of Rolling Stock on the Track to Ensure its Reliability based on the criteria provided in [28]. When determining the permissible speeds for the operation of rolling stock based on track strength conditions, the stresses in the elements of the track superstructure of the specified design are considered when the rolling stock moves at various speeds on straight sections and curves of different radii [29]. As a result, charts similar to Fig. 1 are obtained. When plotting the value of the strength assessment criterion on the graph at the point of its intersection with the calculated value, the permissible speed of the rolling stock is obtained. In Fig. 1, the rolling stock is represented by a wagon with the strength criterion based on stresses in the rails [30].

As a rule, the permissible speed of rolling stock is determined based on the stresses in the rails. If the calculated stresses in other elements of the track superstructure (on the ties, ballast, or main embankment platform) exceed the permissible values, a decision is made to increase their capacity (by increasing the quantity or size) [31, 32]. The maximum stresses in the elements of the track superstructure are determined by the formulas:

- In the base of the rail due to its bending under the action of the moment M:

$$\sigma_0 = \frac{M}{W} = \frac{P_{eq}^{1}}{4kW}, \text{ kg/cm}^2 \quad (1)$$

- In the edges of the rail base:

$$\sigma_k = f\sigma_0, \text{ kg/cm}^2 \quad (2)$$

- In the tie for crushing under the plate (for wooden ties) and in the pad for concrete ties:

$$\sigma_s = \frac{Q}{\omega} = \frac{kl_s}{2\omega} P_{eq}^{II}, \text{ kg/cm}^2 \quad (3)$$

- In the ballast under the tie:

$$\sigma_b = \frac{Q}{\Omega_\alpha} = \frac{kl_s}{2\Omega_\alpha} P_{eq}^{II}, \text{ kg/cm}^2 \quad (4)$$

where:
W: the section modulus of the rail relative to its base, cm³ (Table I);
f: the conversion factor from axial stresses in the rail base to edge stresses, considering the effect of horizontal loads on the rail and the eccentricity of the application of the vertical load [26, 33].

The area of the rail base plate, cm² (Table I). The area of the half-tie, considering the correction for its bending, cm² (Table I).

Table I provides the calculated parameters of the track.

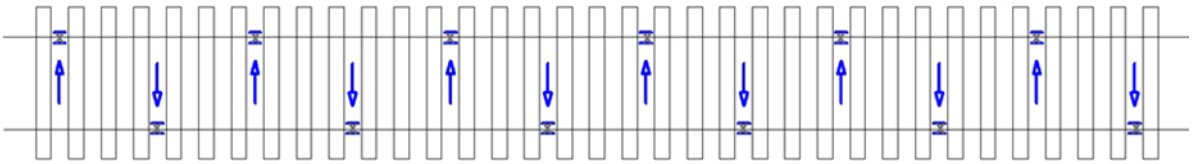

Fig. 5. Sensor placement diagram on the straight track section [32]: ═ Stresses in the lower edges of the rail base; ↑ Lateral forces from the wheel to the rail; **X** – Vertical forces from the wheel to the rail.

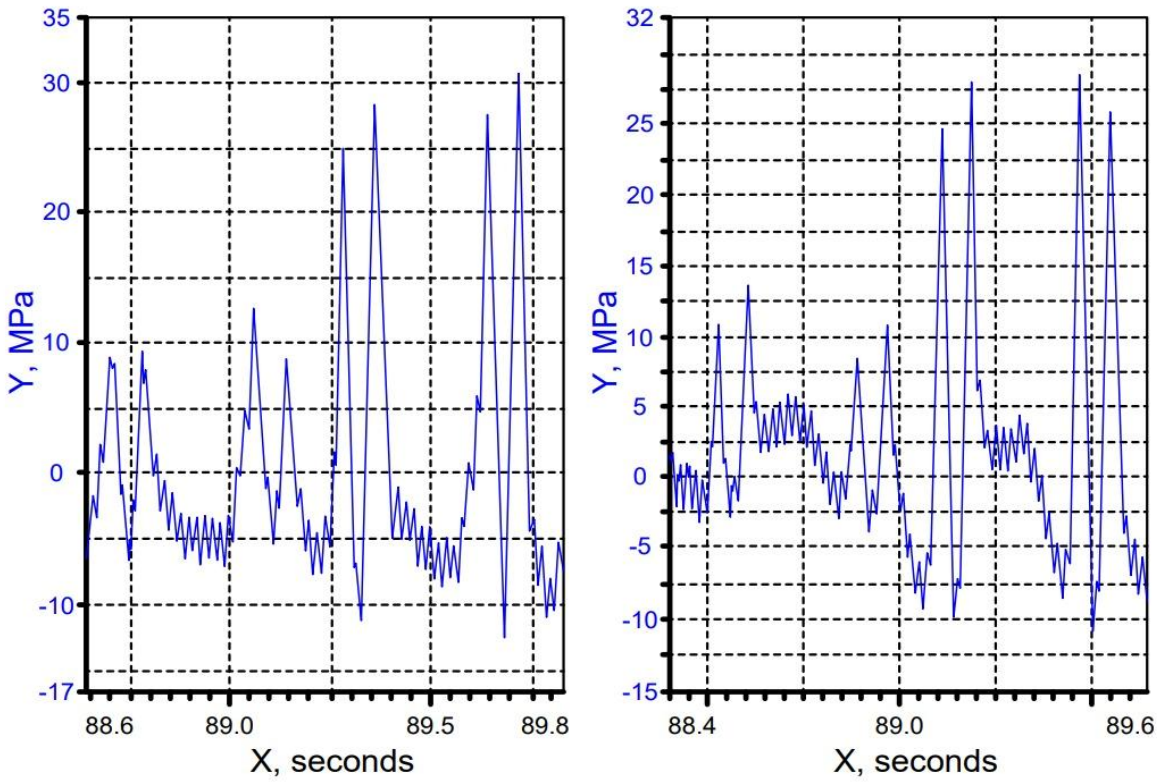

Fig. 6. Stresses in the outer edge of the rail base during the movement of the 12-9920 hopper wagons along the straight track section [26].

TABLE I. CALCULATED TRACK PARAMETERS

Parameter	Values			
Type of rail	R65			
Type of ballast	crushed stone			
Type of sleepers	reinforced concrete		wooden	
Number of sleepers per 1 km of track, pcs/km	1840	2000	1840	2000
Modulus of elasticity of the trackbed, kg/cm²	1500	1670	295	270
The distance between the axes of the sleepers, cm	51	55	51	55
Moment of inertia of the rail at the bottom of the base, cm	417	417	417	417
Area of the half-sleeper with a correction for bending, cm²	3092	3092	2853	2853
Width of the bottom bed of the sleeper, cm	27.6	27.6	25	25
Depth from the sole of the sleeper, cm	55	55	50	50
Cross-sectional area of the rail, cm²	82.65	82.65	82.65	82.65
Moment of inertia of the rail relative to its central horizontal axis, cm⁴	3540	3540	3540	3540
Area of the pad, cm²	518	518	612	612
Distance from the horizontal neutral axis to the outermost heads, cm	9.71	9.71	9.71	9,71
The distance from the horizontal neutral axis to the extreme fibers of the sole of the rail, cm	7.69	7.69	7.69	7,69
Rail head width, cm	7,5	7.5	7.5	7.5
Width of the rail sole, cm	15	15	15	15
Moment of inertia of the rail's cross-section relative to the most distant fiber at the base, cm³	358	358	358	358
Section modulus of the rail's cross-section relative to the most distant fiber at the base, cm³	435	435	417	417

- The calculation formula for determining the normal stresses in the ballast (including on the main platform of the subgrade) at a depth of *h* from the bottom of the sleeper along the design vertical is as follows [34, 35]:

$$\sigma_h = \sigma_{h1} + \sigma_{h2} + \sigma_{h3}, \text{ kg/cm}^2 \quad (5)$$

where:

σ_{h1} and σ_{h3}: the stresses due to the influence of the 1st and 3rd sleepers, respectively, located on both sides of the design sleeper (Fig. 7);
σ_{h2}: the stress due to the influence of the 2nd (design) *sleeper* at the section of the track under the design wheel.

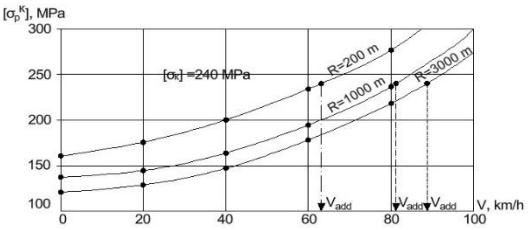

Fig. 7. Stresses at the edges of the rail base of type R50 when a wagon passes.

- The normal vertical stresses under the design sleeper are determined based on the solution of a plane problem in the theory of elasticity, considering the trackbed as a homogeneous isotropic medium, using the following formula:

$$\sigma_{h2} = \sigma_{br}\left[2.55\,C_2 + \left(0.635\,C_1 - 1.275\,C_2\right)m\right] \quad (6)$$

$$C_1 = \frac{b}{2h} - \frac{b^3}{24h^3} \quad (7)$$

$$C_2 = \frac{bh}{b^2 + 4h^2} \quad (8)$$

$$m = \frac{8.9}{\sigma_{br} + 4.35} \geq 1 \quad (9)$$

where:

σ_{br}: the stress under the design sleeper in the ballast, averaged across the width of the sleeper, kg/cm²;
b: the width of the sleeper's bottom plate, cm;
h: the depth of the ballast layer from the bottom of the sleeper, cm;
m: the transition coefficient from the averaged pressure across the width of the sleeper to the pressure under the sleeper's axis, where $m < 1$ is assumed as $m = 1$.

- The stresses at a depth of h under the design sleeper, caused by the influence of adjacent (neighboring) sleepers, are determined using the following formula:

$$\sigma_{h_i} = 0.25\,\sigma_{bc}\,A \quad (10)$$

where $i = 1; 3$

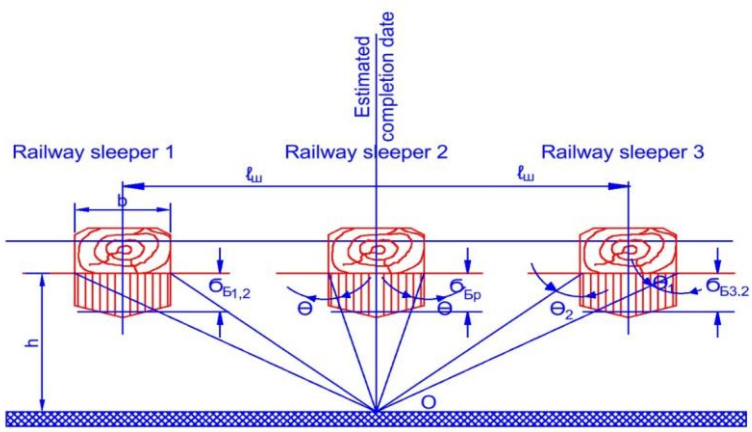

Fig. 8. Diagram of pressure transfer to the subgrade from three adjacent sleepers.

- Considering that the design axis is located above the second (design) sleeper No. 2, the stresses under the first and third sleepers are obtained accordingly [36]:

$$\left.\begin{aligned} \sigma_{h_1} &= 0.25\,\sigma_{Б1,2}\,A \\ \sigma_{h_3} &= 0.25\,\sigma_{Б3,2}\,A \end{aligned}\right\} \quad (11)$$

where:

$\sigma_{Б1,2}$ and $\sigma_{Б3,2}$: the average value of stresses on the sole of the sleepers adjacent to the design one, kg/cm²;

- A is a coefficient that takes into account the distance between the sleepers l_h, the width of the sleeper b and the depth h (see Fig. 8):

$$A = \theta_1 - \theta_2 + 0.5(\sin 2\theta_1 - \sin 2\theta_2) \quad (12)$$

- The angles and (in radians) between the vertical axis and the directions from the edge of the sleeper to the design point (Fig. 7) are determined using the following formulas:

$$\theta_1 = arc\,tg\frac{l_s + 0.5b}{h} \quad (13)$$

$$\theta_2 = arc\,tg\frac{ls - 0.5b}{h} \quad (14)$$

The above formulas are applicable when $h > 15$ cm.

- The stresses in the ballast under the design tie of the b_{br} are determined by the formula:

$$б_{br} = \frac{kl_s}{2\Omega_a} P_{eq}^{II} \quad (15)$$

- In this case, the load of the design wheel located above the design sleeper is calculated using Eq. (15), and the load from the neighboring wheels is calculated using Eq. (16), i.e.:

$$P_{eq}^{II} = P_{dyn}^{\max} + \sum P_{avg}\eta \quad (16)$$

where:

$$\sum P_{avg}\eta = P_{avg}\eta_{l_{1-2}} \quad (17)$$

for a two-axle trolley

- The stresses in the ballast under the sleepers adjacent to the design sleeper are determined based on the condition of the maximum dynamic load of the design wheel located above the design sleeper and the average loads from the other wheels [37]. (Fig. 4):

$$б_{БС} = \frac{kl_s}{2\Omega_a} P_{eq}^{II} \quad (18)$$

where for two-axle bogies:

$$P_{eq}^{II} = P_{dyn}^{\max}\eta_{l_{ш}} + \sum P_{avg}\eta_{(l_{1-2} - l_s)} \quad (19)$$

Under the sleeper №1;

$$P_{eq}^{II} = P_{dyn}^{\max}\eta_{ls} + \sum P_{avg}\eta_{(l_{1-2} + ls)} \quad (20)$$

Under the sleeper №3;

When determining the ordinates, the indices mean:

l_s: the distance between the axes of the sleepers;

l_{1-2} and l_{2-3}: the distances between the 1st, 2nd, and 3rd axes of the bogie, respectively.

Using the above methodology, the stresses in the track structure elements (Figs. 9–11) were calculated for movement on straight and curved track sections. The calculations were performed using the Excel application [38].

Based on the experimental data and the methodology provided above, the stresses in the track structure elements (Figs. 9–11) were calculated for movement on both straight and curved track sections. The calculations were performed using the Excel application [3]. The results of comprehensive tests on freight cars with increased axle load, with models of bogies such as 18-194, 18-9855 Fig. 12, and others, are presented in works [39, 40]. When comparing similar results for the ZK1 bogie, which is installed on the 12-9920 flatcars, the following conclusions can be drawn. The conducted tests showed that the maximum values of interaction forces are more significantly influenced by the design and condition of the rolling stock and track than by the difference in axle load, which, when the load is increased to 25 tons, is 6%, while the variation in the maximum values of dynamic parameters of the cars and their impact on the track can reach up to 30%. The dynamic performance and track impact indicators of the cars with the 18-194, 18-9855, and ZK1 bogies are approximately the same. The greatest negative impact on the railway track is caused by the 18-9996 (ZK1) bogies Fig. 12. Analysis of Figs. 9–11 showed that the stresses in the track structure elements under the action of the hopper car model 12-9920 do not exceed the permissible limits when moving on a track with a typical design [14, 15]. Similarly, calculations were performed for other track structures.

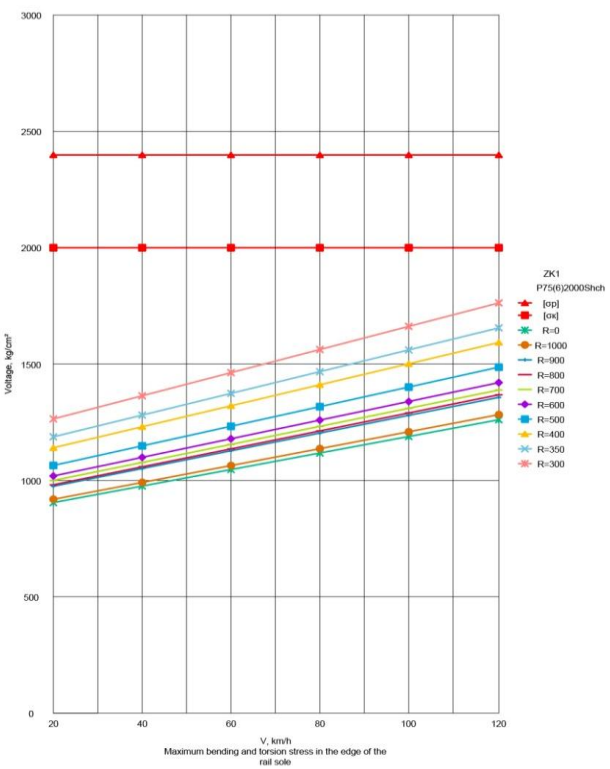

Fig. 9. Maximum bending and twisting stress at the edge of the rail base.

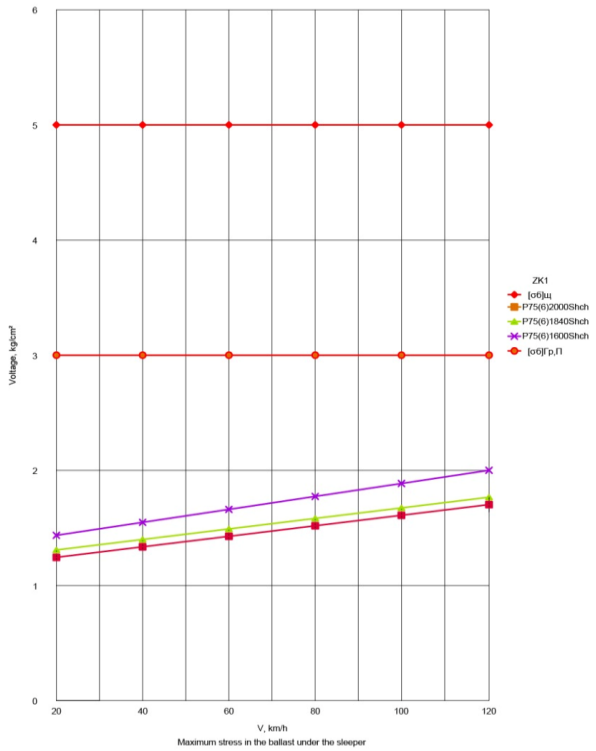

Fig. 10. Maximum stress in the ballast under the sleeper.

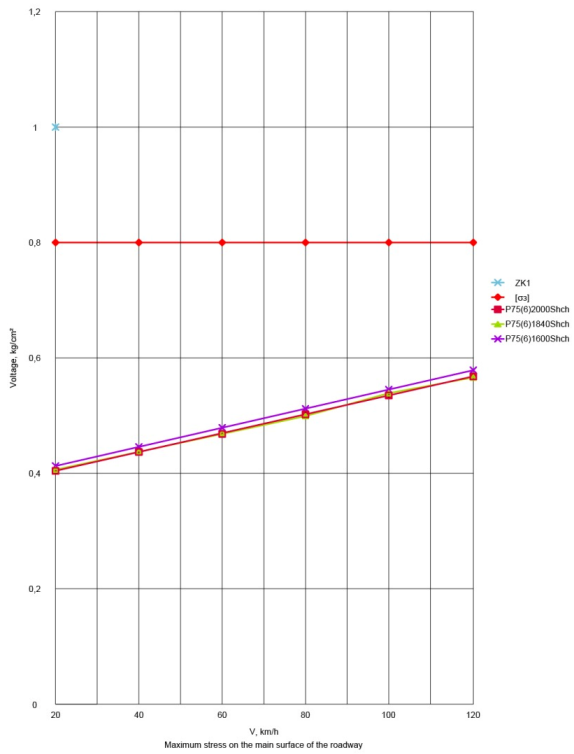

Fig. 11. Maximum stress on the main platform of the subgrade.

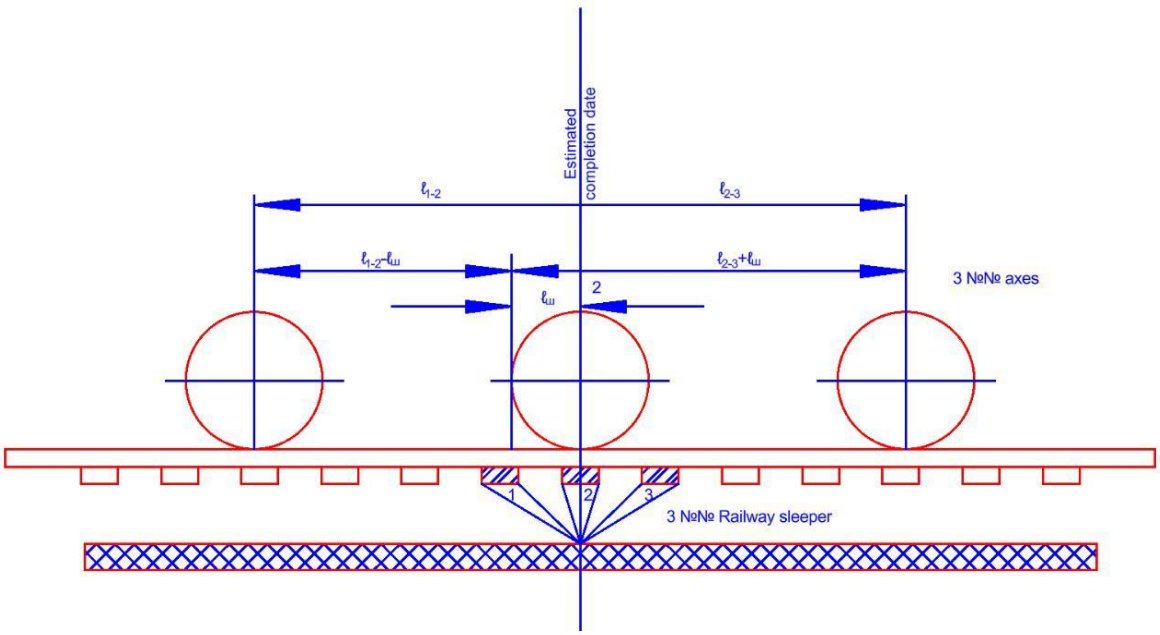

Fig. 12. Consideration of loads from the vehicle axles when determining the stresses on the main platform of the subgrade (for example, the distances from sleeper No. 1, the neighbors of the design sleeper No. 2, to the wheels of the three-axle bogie are shown).

III. Result and Discussion

The experimental section is laid with R65 rails on reinforced concrete ties. The ballast is crushed stone. The tie density is 1840 ties/km. Before the tests on this section, a track measurement wagon was run. According to the measurement results, the maximum allowable speed was determined to be 120 km/h. The straight travel direction for the hopper wagons was assumed when the 12-9920 hopper wagons moved with the first wheelset forward.

The vertical dynamic coefficients of the first and second stages of suspension were determined as the ratio of the dynamic signal values recorded by the strain gauge schemes to the signal value obtained during static tests. The vertical dynamic coefficients were processed without considering the quasistatic component. To measure the accelerations of the truck frames, accelerometers were

installed on the side frames of the hopper wagon trucks above the wheelset axles. To measure the accelerations of the body and the ride quality parameters, accelerometers were installed on the bodies of the hopper wagons at the points where the body rests on the over-spring beam.

Frame forces were measured using calibrated strain gauge schemes, which were glued to the side frames of the hopper wagon trucks. The estimated values of the processed processes were determined as the maximum probable values of the measured values at each speed separately. The estimated values were calculated with a probability of 0.9985.

Based on the data processing results at the specified speed, separate data arrays were formed for each measurement scheme. Using these data arrays, the estimated values of the parameters were found. All measurements were broken down by speed and movement direction. In each run, one maximum amplitude value of the dynamic process was selected. The frame force values were taken into account with the quasistatic component, while the acceleration values were processed without considering the quasistatic component. To evaluate the magnitude of the frame forces, the ratios of the frame forces to the static load from the wheelset on the rails were considered.

Fig. 13 shows the graphs of the dependence of the vertical dynamic coefficient of the first suspension stage on speed during the movement of the hopper wagons along the straight track section [32]. Fig. 14 shows the graphs of the dependence of the vertical dynamic coefficient of the second suspension stage on speed during the movement of the hopper wagons along the straight track section [32]. Fig. 15 shows the graphs of the dependence of the ratio of the frame forces to the static load from the wheelset on the rails to speed during the movement of the hopper wagons along the straight track section [32].

In this and the subsequent figures, the following is indicated:

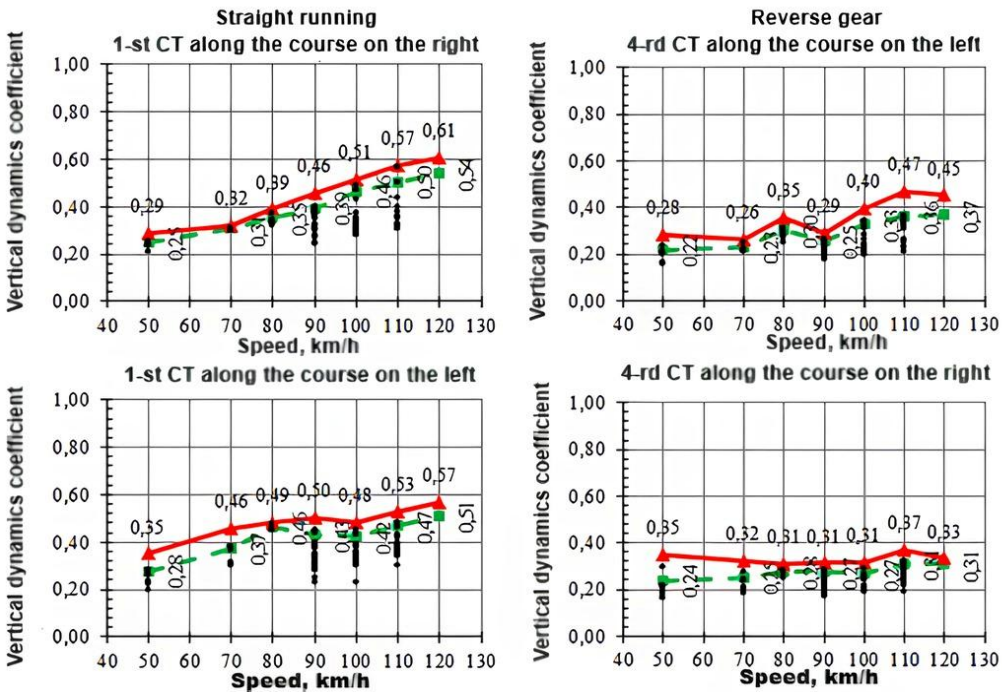

Fig. 13. Vertical dynamic coefficient of the first suspension stage of the loaded 12-9920 hopper wagon during movement along the straight track section [26].

Figs. 10–12 show that the values of the first and second stage vertical dynamic coefficients of suspension, as well as the ratio of frame forces to the static load on the rails of the 12-9920 hopper wagon, do not exceed the allowable limits. Based on the instantaneous values of the frame forces and the first stage vertical dynamic coefficient of the suspension, the stability reserve coefficient against wheel derailment (hereinafter referred to as the KZU) [33, 34] was calculated. The following values for the hopper wagon parameters were used in the calculations:

μ: friction coefficient between the tread of the approaching wheel and the rail, $\mu = 0.25$;

β: the angle of inclination of the wheel tread to the horizontal plane, $\beta = 60^{o}$;

YP: frame force, including the quasi-static component in curved track sections—instantaneous values recorded during each measurement, kN;

Q: gravitational force of the unsprung part of the hopper wagon acting on the wheel axle cheek, $Q = 22.6$ kN for the empty wagon, $Q = 108.8$ kN for the loaded wagon;

Kd1, Kd2: vertical dynamic coefficients for the first stage of suspension (excluding dissipative forces and including the quasi-static component in curved track sections) for the approaching and non-approaching wheels of the wheelset, respectively—these are instantaneous values recorded during each measurement;

μ': friction coefficient between the rolling surface of the approaching wheel and the rail, $\mu' = 0.25$;

q: gravitational force of the unsprung parts applied to the wheelset, q = 18.78 kN;
$2b$: the distance between the points of application of vertical loads to the wheel axle cheeks, $2b$ = 2.036 m;
$a1$: the distance between the point of application of the vertical load on the axle cheek of the approaching wheel and the contact point on the tread, $a1$ = 0.265 m;
$a2$: the distance between the point of application of the vertical load on the axle cheek of the non-approaching wheel and the contact point on its rolling surface, $a2$ = 0.228 m;
r: the radius of the wheel at the rolling circle, r = 0.479 m.

The minimum values of the stability reserve coefficient against wheel derailment, calculated from the data registered on the straight track section, are provided in Table I. As seen from Table I, the minimum value of the stability reserve coefficient against wheel derailment on the straight track section is significantly higher than the regulatory value. Additionally, during dynamic tests, the magnitudes of vertical and horizontal accelerations of the bogies and carriages, as well as the ride smoothness of the 12-9920 model hopper cars, were assessed. It was found that the accelerations of the bogies and carriages, as well as the ride quality indicators, meet the requirements when moving at speeds up to the design speed.

TABLE II. STABILITY RESERVE COEFFICIENT AGAINST WHEEL DERAILMENT ON A STRAIGHT TRACK SECTION

Car	Direction of Movement	Minimum value of the stability margin against derailment (KZU)						
		speed of sideways movement km/h			speed of on a straight track km/h			
		50	70	80	90	100	110	120
Empty hopper car	Straight path	2.70	3.33	2.53	2.63	2.19	2.64	2.38
	Reverse travel	2.38	2.58	2.70	2.40	2.34	2.02	2.19
Loaded hopper car	Straight path	3.22	3.15	2,87	2.98	3.00	3.13	2.97
	Reverse travel	2.92	3.10	2.78	3.10	2.95	3.09	3.06
Permissible value		1.4						

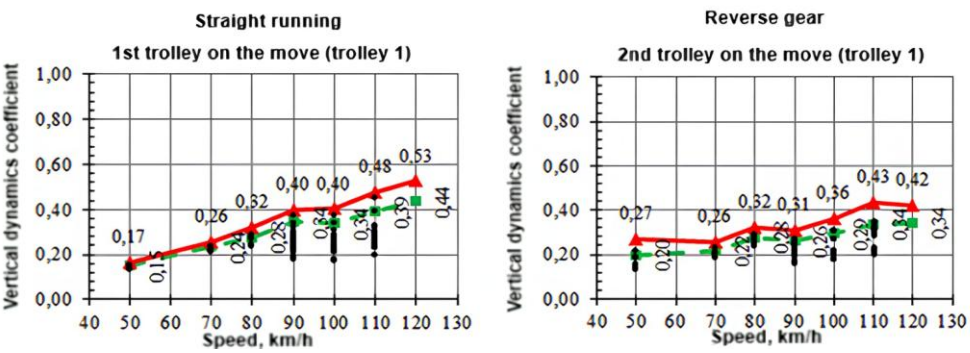

Fig. 14. Vertical dynamic coefficient of the second suspension stage of the loaded 12-9920 hopper wagon during movement along the straight track section [26].

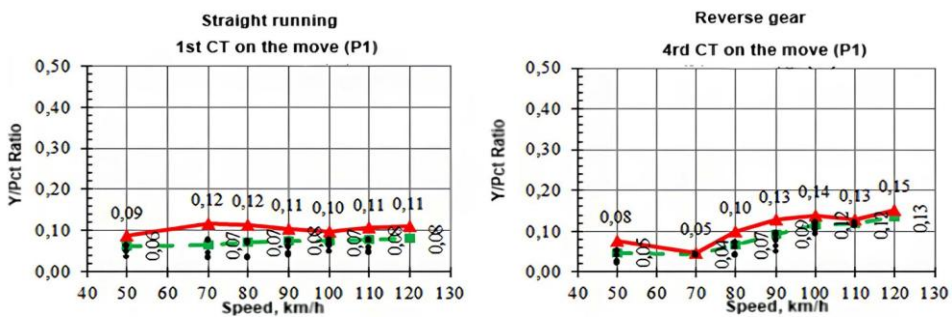

Fig. 15. The ratio of frame forces to the static load from the wheelset on the rails of the loaded 12-9920 hopper wagon during movement along the straight track section [26].

Empirical relationship of the vertical dynamic coefficient of the spring suspension stage with respect to the speed of movement Fig. 16. When calculating stresses in the elements of the track superstructure, an analytical expression is used to describe the relationship between the vertical dynamic coefficient of the spring suspension stage and the speed of movement, based on data obtained from tests [16]. To form this expression, the vertical dynamic coefficients recorded on the guiding bogies were combined into a single data array. The data array included measurement results from both straight sections and curves. For the obtained variation series, the maximum

probable values of the vertical dynamic coefficient (k_d) were calculated for each implemented speed [17].

Based on data processing using the least squares method, this relationship can be described by the empirical formula [18]:

$$\kappa_d = 0.0051\ V + 0.0933 \tag{21}$$

For an empty hopper car:

$$\kappa_d = 0.0034\ V + 0.0207 \tag{22}$$

For a loaded hopper car:
where: V: the speed of movement, km/h.

The given formula is considered valid for the speed range from 25 to 120 km/h.

The obtained dependencies are shown in Figs. 10–12.

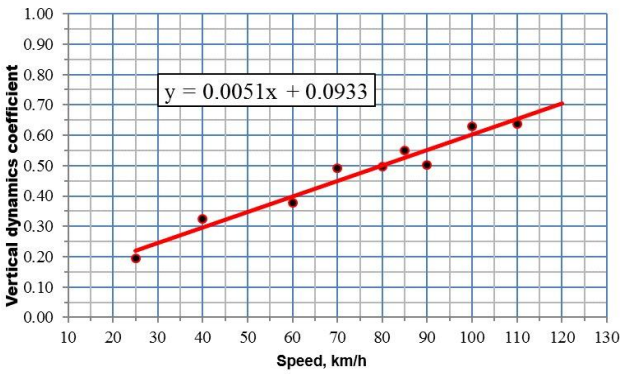

Fig. 16. Generalized dependence of the vertical dynamic coefficient of the spring suspension stage on the speed of movement of the empty hopper car model 12-9920.

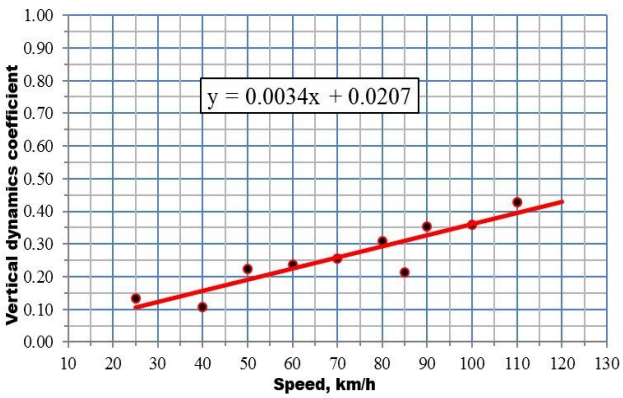

Fig. 17. Generalized dependence of the vertical dynamic coefficient of the spring suspension stage on the speed of movement of the loaded hopper car model 12-9920.

Determination of the permissible speeds for the movement of hopper cars model 12-9920 based on the wheel-rail stability coefficient against derailment Fig. 17. The leading wheels of the bogies of wagons, when moving along curves and often even on straight track sections, may engage with the lateral edges of the rail heads. If the horizontal dynamic pressure force of the wheel on the rail head (RB) is large, and the vertical force (RB) is small Fig. 18. (for example, due to unloading caused by the oscillations of the wagon body), there is a possibility that the flange of the wheel will roll onto the rail head. As the movement continues, the flange rolls onto the rail head, and the wheel may derail. This phenomenon is most commonly observed with empty wagons, where the projection of the force RB1 becomes smaller than the opposing projections of other forces [19, 20].

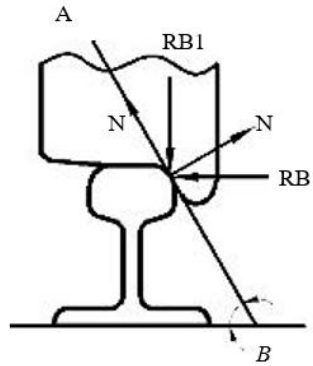

Fig. 18. Coefficient of stability against wheel derailment.

The coefficient of stability against wheel derailment can be determined by the formula [24, 27]:

$$Kyk = \frac{tg\beta - \mu}{1 + \mu \times tg\beta} \times \geqslant [Kyk] \tag{23}$$

where:
β: the angle between the tangent to the surface of the wheel flange and the horizontal, $\beta = 60^{o}$;
μ: the coefficient of friction between the interacting surfaces (the wheel and the rail), $\mu = 0.25$.

The results of the experimental data processing showed that the dynamic indicators characterizing the running performance of the hopper car model 12-9920 do not exceed the permissible values [29]. The following parameters are within the standard limits:

- The coefficient of the transverse stability margin of the wagon against overturning when moving on curved sections of the track;
- Body accelerations in vertical and horizontal transverse directions in both empty and loaded states of the wagon;
- The coefficient of the structural margin for the deflection of the spring suspension, considering the maximum load from the axle to the rails;
- The coefficients of the stability margin of the wheel against derailment for all confidence probabilities (Table II) [15, 21].

Table III presents the permissible speeds for the movement of the hopper car model 12-9920, the following conditional symbols in the form of letters are used to the left of the permissible speed values:
K: the design speed of the rolling stock;
H: the permissible speed of the rolling stock, established by the value of the accepted unattenuated acceleration on curved sections of the track, with the outer rail elevated by 150 mm.

TABLE III. EXPERIMENTAL DATA ON THE ESTIMATION OF THE COEFFICIENT OF STABILITY OF THE WHEEL FROM DERAILMENT

The coefficient of stability of the wheel from derailment	Acceptable probability, no more than	Actual probability	
		Empty carriage	Loaded carriage
1.15	0.0001	<0.00001	<0.00001
1.25	0.0001	0.00007	<0.00001
1.45	0.001	0.00098	0.00086
1.6	0.01	0.00551	0.00282

As seen from Table IV, the operation of 12-9920 model flatcars at a speed of 120 km/h is permitted on straight sections of track of standard design (rails R65, ballast—crushed stone/asbestos, sleeper spacing of at least 1840 per km) and on curves with radii not less than 600 m. When the 12-9920 flatcars move on curves with radii less than 600 m, the maximum speed must be limited by the magnitude of the uncompensated acceleration. When moving on tracks that differ from the standard design, the speed of the 12-9920 model flatcars is limited by the standards for the permissible maximum stresses in the elements of the track structure and on the main platform of the earthwork. The obtained permissible speeds allow for the safe operation of the 12-9920 model flatcars on the railways of Kazakhstan. The results of experimental studies can be used to calculate the stress-strain state of continuously welded track and to optimize the rolling stock of freight cars with increased axle loads.

TABLE IV. PERMISSIBLE SPEEDS FOR THE MOVEMENT OF HOPPER CARS MODEL 12-9920

Type of rails; reduced wear of the rail head in mm; number of sleepers per 1 km; type of ballast	Direct	Permissible speeds, km/h				Radius of curves, m			
		1000	800	700	600	500	400	350	300
R65(6) 2000, 1840 CS, As and harder	120	120	120	120	120	H-85	H-80	H-70	H-65
R65(6) 2000, 1840 Gr and harder	100	100	100	90	80	80	H-80	H-70	H-65
R50(6) 2000, 1840 CS, As, Gr, S	75	75	75	75	75	75	75	H-70	H-65
R50(6) 1600 CS, As, Gr	65	65	65	65	65	65	65	65	65
R50(6)2000, 1840 S	75	75	75	75	75	75	75	H-70	H-65
R50(6)1600 S	65	65	65	65	65	65	65	65	55
R43(6)1840 CS, As	65	65	65	65	65	60	50	45	35
R43(6)1600 CS, As	60	60	60	60	60	60	45	35	25
R43(6)1840 Gr	70	70	70	70	65	60	45	40	25
R43(6)1600 Gr	60	60	60	55	50	45	40	35	20
R43(6)1840	55	55	55	55	50	45	40	30	20
R43(6)1600 S	45	45	45	45	45	40	30	20	10

IV. CONCLUSION

The development of heavy freight traffic in Kazakhstan poses challenges for increasing axle loads. In this context, the introduction of cars with increased load capacity requires research aimed at establishing safe operating conditions for rolling stock and ensuring the stability of the railway infrastructure [35]. During the dynamic testing of flatcars, dynamic indicators were assessed, including the vertical dynamic coefficient, wheel stability against derailment, and the lateral and vertical forces acting from the wheel on the rail. It was determined that the maximum values of the dynamic indicators do not exceed the normative permissible levels when operating on a standard track.

Based on experimental data, the maximum axial stress in the rail foot due to its bending was obtained. This parameter serves as the initial parameter for calculating the strength of the railway track. Using the commonly accepted methodology, stresses in the elements of the track structure and on the main platform of the earthwork were determined, which allowed for the justification of the permissible operating speeds of the 12-9920 model flatcars on railways of different designs [36].

The permissible speed for the 12-9920 model flatcar when moving on standard track designs on straight sections and large-radius curves (up to 600 m inclusive) can be set at the design speed (120 km/h). For movement on small-radius curves, the permissible speed must be determined based on the limitation of uncompensated acceleration [37, 38]. The permissible speed for the 12-9920 model flatcar when moving on other track designs should be determined based on the limitation of uncompensated acceleration as well as the track strength criterion. The methodology is based on calculations of dynamic characteristics and modeling of the interaction of rolling stock with track infrastructure [41]. The results can be applied in the design of railway transport, the modernization of rolling stock and the development of regulatory documentation to ensure traffic safety.

CONFLICT OF INTEREST

The authors declare no conflict of interest.

AUTHOR CONTRIBUTIONS

SA and DK organization and management of research, writing of the manuscript; AA experimental work, computer processing and correction of the manuscript, communication with the editorial board of the journal; AK, AT assistance with computer processing of the manuscript; AB and DK literature review and analysis of methods; NT-K, AT analysis of methods and execution of calculations; all authors had approved the final version.

REFERENCES

[1] M. F. Verigo, "Vertical forces acting on the track during the passage of rolling stock," in *Proc. Central Sci. Res. Inst. Ministry Railways*, no. 97, Moscow, Russia, 1955, pp. 25–26.

[2] G. Imasheva *et al.*, "Prospects for the use of gondola cars on bogies of model ZK1 in the organization of heavy freight traffic in the Republic of Kazakhstan," *Mechanika*, vol. 24, no. 1, pp. 32–36, 2018. doi: 10.5755/j01.mech.24.1.17710

[3] S. Abdullayev, N. Tokmurzina, and G. Bakyt, "The determination of admissible speed of locomotives on the railway tracks of the Republic of Kazakhstan," *Transport Problems*, vol. 11, no. 1, pp. 61–68, 2016.

[4] S. Abdullayev *et al.*, "Interaction of the TE33A diesel locomotive and the railway track on curved sections with a radius of 290 m," *Commun.-Sci. Lett. Univ. Žilina*, vol. 25, no. 4, 410, 2023. doi: 10.26552/com.C.2023.069

[5] S. Abdullayev *et al.*, "Dynamic interaction of the TE-33A diesel locomotive and the track in a curve with a radius of 600 meters," *Int. J. Mech. Eng.*, vol. 13, no. 2, pp. 205–212, 2023. doi: 10.18178/ijmerr.13.2.205-212

[6] A. Lau and I. Hoff, "Simulation of train-turnout coupled dynamics using a multibody simulation software," *Model. Simul. Eng.*, vol. 2018, pp. 1–10, 2018, doi: 10.1155/2018/8578272

[7] S. Bruni *et al.*, "Modelling of suspension components in a rail vehicle dynamics context," *Veh. Syst. Dyn.*, vol. 49, no. 7, pp. 1021–1072, 2011. doi: 10.1080/00423114.2011.586430

[8] P. M. Jawahar, K. N. Gupta, and E. Raghu, "Mathematical modelling for lateral dynamic simulation of a railway vehicle with conventional and unconventional wheelset," *Math. Comput. Model.*, vol. 14, pp. 989–994, 1990. doi: 10.1016/0895-7177(90)90326-I

[9] A. Abdykadyrov *et al.*, "Research of the process of ozonation and sorption filtration of natural and anthropogenicly pollated waters," *J. Environ. Manage. Tourism*, vol. 14, no. 3, pp. 811–822, 2023. doi: 10.14505/jemt.v14.3(67).20

[10] A. Abdykadyrov *et al.*, "Purification of surface water by using the corona discharge method," *Min. Mineral Deposits*, vol. 18, no. 1, pp. 125–137, 2024. doi: 10.33271/mining18.01.125

[11] A. Orlova and Y. Boronenko, "The anatomy of railway vehicle running gear," in *Handbook of Railway Vehicle Dynamics*, S. Iwnicki, Ed. Boca Raton, FL, USA: CRC Press, 2006, pp. 39–84.

[12] S. S. Abdullayev *et al.*, "Interaction of frame structures with rolling stock," *News Natl. Acad. Sci. Republic Kazakhstan, Ser. Geol. Tech. Sci.*, vol. 445, no. 1, pp. 22–28, 2021. doi: 10.32014/2021.2518-170X.3

[13] S. Abdullayev *et al.*, "Simulation of spring-friction set of freight car truck, taking into account track profile," *Int. J. Innov. Res. Sci. Stud.*, vol. 7, no. 2, pp. 755–763, 2024. doi: 10.53894/ijirss.v7i2.2883

[14] E. Di Gialleonardo, S. Bruni, and H. True, "Analysis of the nonlinear dynamics of a 2-axle freight wagon in curves," *Veh. Syst. Dyn.*, vol. 52, no. 1, pp. 125–141, 2014. doi: 10.1080/00423114.2013.863363

[15] N. Bosso, M. Magelli, and N. Zampieri, "Dynamical effects of the increase of the axle load on European freight railway vehicles," *Appl. Sci.*, vol. 13, no. 3, 1318, 2023. doi: 10.3390/app13031318

[16] G. D. Mpye and P. J. Gräbe, "The effect of increased axle loading on the behavior of heavily overconsolidated railway foundation materials," *Transp. Geotech.*, vol. 27, 100493, 2021. doi: 10.1016/j.trgeo.2020.100493

[17] I. S. Besedin, L. A. Muginshtejn, and S. M. Zaharov, "The development of heavy traffic on the railways of the world," *Railways World*, no. 9, pp. 39–48, 2006.

[18] O. A. Shykunov, "Three-element bogie side frame strength," *Sci. Prog. Transp. Bull. Dnipro Nat. Univ. Railway Transp.*, vol. 1, no. 67, pp. 183–193, 2017.

[19] Y. P. Boronenko, A. V. Tretyakov, and M. V. Zimakova, "Evaluation of the possibility and efficiency of increasing axle loads of freight wagons," *Bull. Inst. Nat. Monopolies: Railway Eng.*, no. 1, pp. 32–37, 2017.

[20] N. A. Tokmurzina-Kobernyak, N. V. Ivanovtseva, and A. K. Makhanova, "Dynamic interaction parameters of tracks of freight wagons with increased axle load," *Bull. KazATC*, vol. 1, no. 1, pp. 109–115, 2019.

[21] L. Sun, "Dynamic displacement response of beam-type structures to moving line loads," *Int. J. Solids Struct.*, vol. 38, pp. 8869–8878, 2001.

[22] S. Bhardawaj, R. C. Sharma, and S. K. Sharma, "A survey of railway track modelling," *Int. J. Vehicle Struct. Syst.*, vol. 11, no. 5, pp. 508–518, 2019. doi: 10.4273/ijvss.11.5.08

[23] Z. Major *et al.*, "Dynamic modeling possibilities of embedded rail structures," *Acta Polytech. Hung.*, vol. 22, no. 4, pp. 29–43, 2025. doi: 10.12700/APH.22.4.2025.4.3

[24] J. Eisenmann, "Slab track for railways," in *Betonkalender*, vol. 2, 2000, pp. 291–326. (in German)

[25] J. Eisenmann, "The rail as a supporting beam," The Railway Engineer, vol. 55, pp. 22–25, 2004.

[26] S. Abdullayev, N. Tokmurzina, and G. Bakyt, "The determination of admissible speed of locomotives on the railway tracks of the Republic of Kazakhstan," *Transport Problems*, vol. 11, no. 1, pp. 61–68, 2016. doi: 10.20858/tp.2016.11.1.6

[27] P. Wu *et al.*, "Review of wheel-rail forces measuring technology for railway vehicles," *Adv. Mech. Eng.*, 2023, doi: 10.1177/16878132231158991

[28] A. M. Brzhezovskiy, "Proposals for development of a reference method for measuring lateral forces," *Russ. Railway Sci. J.*, vol. 81, no. 2, pp. 101–113, 2022, doi: 10.21780/2223-9731-2022-81-2-101-113

[29] S. Abdullayev, A. Izbairova, A. Abdullayeva, A. Tursynbayeva, and G. Bakyt, "The forces exerted by the TE33A locomotive on the switch elements," *Int. J. Innov. Res. Sci. Stud.*, vol. 8, no. 3, pp. 2534–2544, 2025. doi: 10.53894/ijirss.v8i3.7050

[30] S. A. Kosenko *et al.*, "Field measurements of rail stresses under the influence of rolling stock," *J. Transsib Railway Stud.*, vol. 30, no. 2, pp. 133–145, 2017.

[31] H. Song *et al.*, "Study on the steel rail rolling contact stress with consideration of initial residual stress," in *Proc. MATEC Web Conf.*, 2015, vol. 22, 03018. doi: 10.1051/matecconf/20152203018

[32] K. Zhussupov *et al.*, "Investigation of the stress-strain state of a wheel flange of the locomotive by the method of finite element modeling," *Mechanika*, vol. 24, no. 2, pp. 174–181, 2018. doi: 10.5755/j01.mech.24.2.17637

[33] S. Abdullayev, "The TE33A series diesel locomotive brake equipment tests," *Commun.-Sci. Lett. Univ. Žilina*, vol. 26, no. 3, pp. B142–B154, 2024. doi: 10.26552/com.C.2024.029

[34] S. Abdullayev *et al.*, "Testing of railway equipment for the impact on the track and turnouts," *Commun.-Sci. Lett. Univ. Žilina*, vol. 26, no. 2, pp. B99–B107, 2024. doi: 10.26552/com.C.2024.020

[35] K. Uylan, M. Gokasan, and S. Bogosyan, "Analysis of stability and derailment of high-speed railway vehicles moving on curved tracks," *Int. J. Heavy Vehicle Syst.*, vol. 26, no. 6, pp. 824–853, 2019. doi: 10.1504/IJHVS.2019.102685

[36] Y. S. Romen *et al.*, "Establishing conditions for the operation of wagons with increased axle load," *Transp. Russian Federation*, no. 3, pp. 39–48, 2013.

[37] A. M. Orlova *et al.*, "On the determination of permissible speeds for railway rolling stock on the Russian Federation's railway network," *Vestnik Inst. Nat. Monopolies: Railway Eng.*, no. 3, pp. 52–60, 2019.

[38] H. M. Sedighi and K. H. Shirazi, "Bifurcation analysis in hunting dynamical behavior in a railway bogie: Using novel exact figequivalent functions for discontinuous nonlinearities," *Scientia Iranica*, vol. 19, no. 6, pp. 1493–1501, 2012. doi: 10.1016/j.scient.2012.10.028

[39] G. Bakyt *et al.*, "Simulation of dynamic processes of interaction of car and railway track during train passage of curved sections of the track," *Transp. Problems*, vol. 15, no. 2, pp. 45–70, 2020. doi: 10.21307/tp-2020-020

[40] R. Konovrotski and A. Hoinacki, "Analysis of operational reliability of railway vehicles in terms of safety against derailment based on various methods of determining the evaluation criteria," *Eksploat. Niezawodn.*, vol. 22, no. 1, pp. 73–85, 2020.

[41] S. Abdullayev, "The TE33A series diesel locomotive brake equipment tests," *Commun.-Sci. Lett. Univ. Žilina*, vol. 26, no. 3, pp. B142–B154, 2024. doi: 10.26552/com.C.2024.029

Copyright © 2025 by the authors. This is an open access article distributed under the Creative Commons Attribution License which permits unrestricted use, distribution, and reproduction in any medium, provided the original work is properly cited (CC BY 4.0).